On the Potential for Multiscale Oscillatory Behavior in HIV

Alexander V. Ratushny [1]

Email alexander.ratushny@cidresearch.org

Patrick De Leenheer [2]

Email deleenhp@science.oregonstate.edu

Sergei I. Bazhan [3]

Email bazhan@vector.nsc.ru

Gennady A. Bocharov [4]

Email bocharov@m.inm.ras.ru

Tamara M. Khlebodarova [5]

Email tamara@bionet.nsc.ru

Vitaly A. Likhoshvai [5,6]

Email likho@bionet.nsc.ru

[1] The Center for Infectious Disease Research (formerly Seattle Biomedical Research Institute) and Institute for Systems Biology, Seattle, WA, USA

[2] Oregon State University, Corvallis, OR, USA

[3] State Research Center of Virology and Biotechnology “Vector”, Koltsovo, Russia

[4] Institute of Numerical Mathematics, Russian Academy of Sciences, Moscow, Russia

[5] Institute of Cytology and Genetics, Siberian Branch of the Russian Academy of Sciences, Novosibirsk, Russia

[6] Novosibirsk State University, Novosibirsk, Russia

Abstract

The abstract is published online only. If you did not include a short abstract for the online version when you submitted the manuscript, the first paragraph or the first 10 lines of the chapter will be displayed here. If possible, please provide us with an informative abstract.

This chapter summarizes several theoretical studies on the potential for oscillatory behavior of HIV infection at molecular and cellular levels. It discusses the biological relevance of oscillatory systems in the HIV life cycle and touches upon broader perspectives for further theoretical and experimental exploration of system dynamics. The potential interference of HIV oscillatory dynamics at different multiscale levels as well as interaction and coevolution with the complex host immune system is also discussed.

Keywords

HIV
Mathematical kinetic model
Systems biology
Multiscale system
Oscillatory dynamics
Host-pathogen interaction
Differential equation
Coevolution
Intracellular
Population dynamics

Core Message

Nonlinear dynamics and inherently multiscale properties of the HIV-host system impede our ability to effectively intervene in the disease process. Bursty or oscillatory behavior of the virus along with its other strategies to avoid elimination by the host immune system has significant implications for diagnosis and control of infection. Mathematical modeling of HIV-host multiscale interactions and dynamics offers an opportunity to coherently integrate available experimental data, reveal nontrivial emergent properties of the system, and systematically explore optimal intervention strategies.

AQ1

34.1. Introduction

The life cycle of human immunodeficiency virus type 1 (HIV-1) is complex and inherently multiscale [1, 2]. The virus has developed various strategies to avoid elimination by the host immune system [3, 4, 5, 6]. These strategies result in intricate dynamical behaviors of the host-virus system. HIV-1 exploits the host organism at multiple levels during the course of infection. In this chapter, we discuss two levels of host-virus dynamical interactions. Namely, we consider the within-host organism and the within-host target cell (e.g., T cells or macrophages) HIV dynamics (Fig. 34.1). Within-host organism HIV dynamics represents the host-virus interaction at the cell population level (Fig. 34.1A), whereas within-host target cell HIV dynamics represents the host-virus interaction at the intracellular level (Fig. 34.1B). These two scales of host-virus interactions are tightly interlinked and shape the overall dynamical properties of the host-virus system.

Fig. 34.1

Schematic representation of the link between the within-host organism and within-host target cell HIV dynamics. (*A*) The within-host organism HIV dynamics is considered at the cell population level. (*B*) The within-host target cell HIV dynamics is considered at the intracellular level. Uninfected target cells (e.g., T cells or macrophages) can be infected by viruses and converted to latently or productively infected target cells. HIV dynamics at both scales are intertwined and interdependent

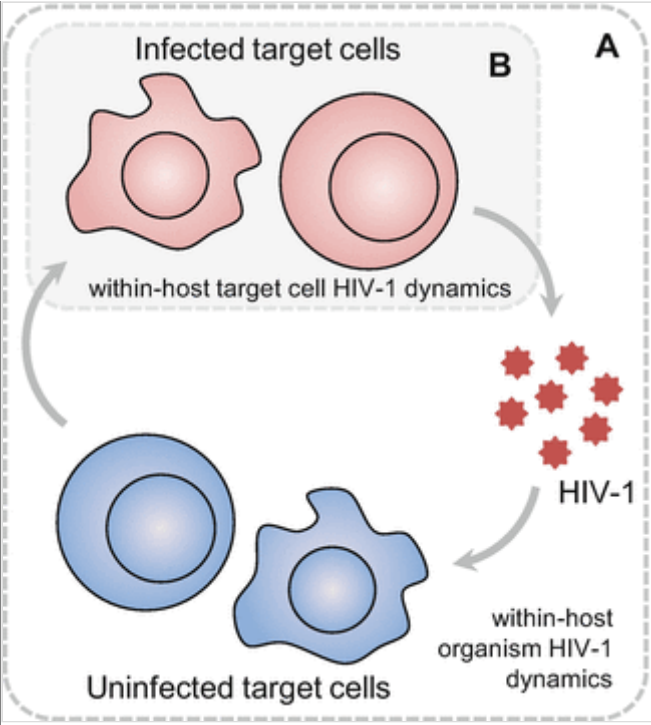

The host-HIV interaction at the cell population level can be viewed and modeled as a collection of different target cell types with different properties (e.g., half-lives, probabilities of being infected), which can be infected by HIV and converted to infected cells also with different properties (e.g., latently or productively infected) [7]. The host-HIV interaction models at the cell population level can be used to systematically analyze the rates of HIV infection and replication, the rate of HIV particle clearance, and different properties of infected cells [7, 8, 9] and to explore intervention strategies and appearance of drug-resistant virus populations [10, 11].

The host-HIV interaction at the intracellular level can be viewed and modeled as a system of interacting host and HIV molecular components within the target cell [12, 13, 14, 15, 16, 17]. The intracellular host-HIV interaction models can be used for systematic analysis of the transient properties of the viral replication processes, such as, reverse transcription, integration of proviral DNA into the host genome, transcription, RNA maturation and transport from the nucleus to the cytoplasm, synthesis and transport of viral proteins to the cell membrane, and viral particle assembly. There are multiple nonlinear molecular mechanisms of intracellular HIV-1 replication. One such mechanism is positive regulation of virus replication by Tat protein via the antitermination of genomic RNA transcription on the trans-activation response (TAR) element of the proviral DNA (Fig. 34.2). Another mechanism is based on interference with the splicing of full-length (9 kb) RNA and incompletely spliced (4 kb) RNA molecules through their active transport from the nucleus to the cytoplasm [18]. The Tat and Rev proteins are synthesized by infected cells at early stages of HIV-1 ontogenesis. Their mRNAs are fully spliced (2 kb) RNAs [19] and can be transported into the cytoplasm without delay by RNA transport machinery [18]. The production of the Tat protein leads to an augmentation of full-length genomic RNA transcription by at least 25- to 100-fold [20, 21, 22, 23, 24, 25]. This full-length HIV-1 genomic RNA encodes Gag and Gag-Pol proteins, which are essential for the formation of virus particles in the cytoplasm [26]. Since there are no molecular mechanisms of nuclear-cytoplasmic transport of intron-containing RNA in the cells of higher organisms, the export of intron-containing RNA to the cytoplasm is mediated by HIV-1 Rev proteins (Fig. 34.2). The Rev protein contains a nuclear localization sequence (NLS) and a nuclear export sequence (NES), which control the shuttling of Rev between the nucleus and cytoplasm [27, 28]. Its appearance in the nucleus followed by an interaction with the Rev response element (RRE) leads to the assembly of a high-affinity complex on unspliced (9 kb) or incompletely spliced (4 kb) viral mRNA [29] and the export of the above classes of the viral mRNAs out of the nucleus. This results in a downregulation of the generation of the completely spliced mRNAs and, therefore, the overall synthesis of the Rev and Tat proteins [30].

Fig. 34.2

Schematic representation of the regulation of HIV-1 replication by Tat and Rev, *dotted arrows* represent a positive regulation. *Dotted oval arrow* represents a negative regulation. The description of the numbered processes is presented in the text (Modified from Likhoshvai et al. [17])

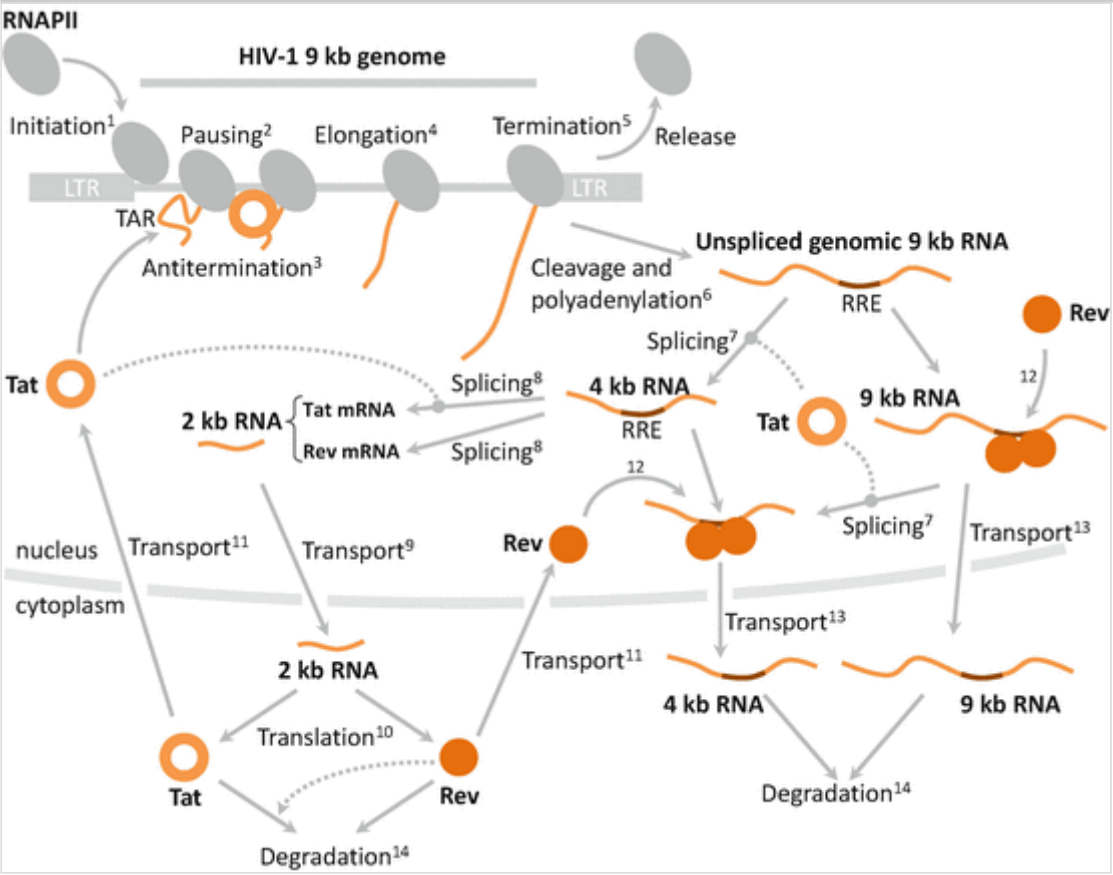

34.2. Network Motifs for Oscillatory Behavior of Within-Host Organism and Within-Host Target Cell HIV Dynamical Systems

There are positive and negative feedback loops in the within-host organism and within-host target cell HIV dynamical systems (Fig. 34.3). At the cell population level, HIV-1 enhances its viral titer by infecting the target cells and converting them into productively infected cells. At the same time, HIV is actively reducing the number of uninfected target cells that can be viewed as an indirect negative feedback regulation (Fig. 34.3a). At the intracellular level, the positive feedback loops are dictated by the self-replicating molecular mechanisms of the virus [31]. One of the positive feedback loops is the transcriptional activation of HIV-1 components including Tat-encoding mRNA by Tat through TAR element. There is also a negative feedback regulation of Tat and Rev mRNA synthesis by Rev (Figs. 34.2 and 34.3b). Moreover, the negative feedback loop in this system is reinforced by the negative regulation of tat mRNA synthesis in the nucleus by the Tat protein through inhibition of splicing 9 kb and 4 kb RNAs to 2 kb mRNAs encoding Tat as well as by the positive regulation of the Tat protein degradation in the cytoplasm by Rev and the HIV nucleocapsid protein (NC) [32, 33, 34]. NC is translated from the full-length viral genomic RNA as a part of the Gag polyprotein and subsequently processed by a viral protease.

Fig. 34.3

Positive and negative feedback loops in the within-host organism (**a**) and within-host target cell (**b**) HIV dynamical systems. *Red solid and dashed arrows* represent direct and indirect, respectively, positive regulation. *Blue oval dashed arrows* represent indirect negative regulation

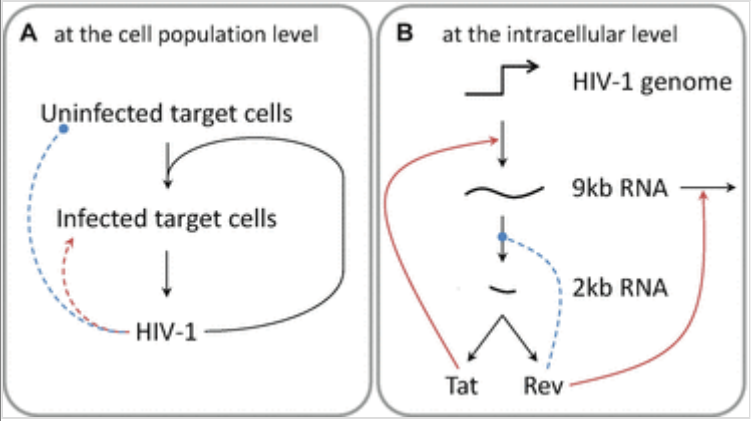

It is known that molecular regulatory systems with negative feedback loops or network architectures comprising linked positive and negative feedback loops can potentially have an oscillatory behavior or a limit cycle [35, 36, 37, 38, 39]. There are multiple theoretical studies of both natural and synthetic gene regulatory networks that demonstrate an important role for negative feedback loops in the oscillatory behavior of the system [40, 41, 42, 43, 44]. Examples of such systems include oscillation of NF-κB protein in the immune response [45, 46, 47], the oscillatory behavior of Hes1 and Hes7 proteins and their regulation of the formation of somites in developing vertebrate embryos [48, 49], and the oscillation of p53 and its regulation of apoptosis [50]. Thus, the regulatory program of HIV-1 ontogenesis has all of the prerequisites for oscillatory regimes in the production of viral particles at both the cell population and intracellular scales. In this chapter we will briefly review mathematical models of the within-host organism and within-host target cell HIV dynamical systems and describe theoretical results that support the existence of oscillatory dynamics of HIV-1 at both scales.

34.3. Sustained Oscillations in the Basic Within-Host Organism HIV Model

One of the early within-host organism models, known as the standard model, was used by Perelson and Nelson [51] and by Nowak and May [52] to model HIV. It was successful in numerically reproducing of early stages of the HIV lifecycle in its target, the CD4+ T cells, following an infection event. The global behavior of the standard model was first investigated analytically in [53] and will be reviewed here. The global stability of a disease steady state was proved under certain conditions, using powerful second compound matrix methods developed by Muldowney [54] and by Li and Muldowney [55]. It also established the possibility of sustained oscillations in particular regions of the parameter space.

After HIV enters its target, a *T* cell, it makes a DNA copy of its viral RNA. The viral DNA is then inserted into the DNA of the *T* cell, which will henceforth produce viral particles that can bud off the cell to infect other uninfected *T* cells. A concise summary in chemical reaction notation of these processes is

$$T + V \rightarrow T^* \rightarrow NT$$

where *N* is the expected number of viral particles that bud off an infected *T* cell over its lifetime. These mathematical models assume mass action kinetics for both of the reactions above.

The standard model has three state variables: *T*, the concentration of uninfected *T* cells; *T**, the concentration of productively infected *T* cells; and *V*, the concentration of free virus particles in the blood. The interaction between these cells and virus particles is then given by the following equations [51, 52, 53]:

$$\dot{T} = f(T) - kVT \qquad 34.1$$

$$\dot{T^*} = kVT - \beta T^* \tag{34.2}$$

$$\dot{V} = N\beta T^* - \gamma V - kVT \tag{34.3}$$

The functional form of f is defined differently by different authors:

1. Perelson and Nelson [51] take

$$f(T) = f_1(T) = \delta - \alpha T + pT\left(1 - \frac{T}{T_{\max}}\right).$$

2. Nowak and May [52] use $f(T) = f_2(T) = \delta - \alpha T$.

The parameters α, β, γ , δ, k, N, p, and $T_{\max}$ are positive and have the following interpretation:

1. α, β, and γ are death rates for uninfected T cells, infected T cells, and virus particles, respectively.
2. k is the contact rate between uninfected T cells and virus particles.
3. δ represents a constant production of T cells in the thymus.
4. N is the average number of virus particles produced by an infected T cell during its lifetime.
5. In the case $f = f_2$, healthy T-cell proliferation is neglected, and only the thymus serves as a source of newly produced healthy T cells. In the case $f = f_1$, healthy T cells are assumed to proliferate logistically. The parameters p and $T_{\max}$ are the growth rate and carrying capacity, respectively, associated with a logistic growth of uninfected T cells in the absence of virus particles, infected T cells, and other sources such as the thymus. This logistic proliferation is a simplification of the more biologically realistic term $pT\left(1 - \frac{T+T^*}{T_{\max}}\right)$, and a model that includes this term instead has since been considered in [56]. Another simplification is that logistic proliferation of the infected T cells has been neglected, but this has also been considered since then, namely, in [57].

The simplifications regarding T-cell proliferation have important mathematical consequences, because the resulting system turned out to be a three-dimensional competitive system [58], which opened up a whole arsenal of tools to analyze the model [53].

The model always has a disease-free steady state $E_0 = (T_0, 0, 0)$, where T_0 is the positive root of the function f, i.e., $f(T_0) = 0$. There may be a second, chronic disease steady state $E_e = (T_e, , T_e^*, , V_e)$, if and only if the value of the basic reproduction number

$$R_0 = \frac{kNT_0}{\gamma + kT_0}$$

is larger than 1.

If $R_0 > 1$, then E_0 is unstable, and Smith and De Leenheer [53] provide conditions under which E_e is globally stable.

However, when $f = f_1$, there exist regions in parameter space (e.g., when kT_{max} and p are sufficiently large, see [53]), where E_e is unstable with a two-dimensional unstable manifold (caused by the linearization having a pair of imaginary eigenvalues with positive real part), and a one-dimensional stable manifold (by the linearization having a real, negative eigenvalue). In this case, there exists at least one orbitally asymptotically stable periodic orbit. Every solution, except those with initial data on the one-dimensional stable manifold of E_e or on the invariant T-axis, converges to a nontrivial periodic orbit. In other words, in this case, the model exhibits sustained oscillations (Fig. 34.4).

Fig. 34.4

Periodic solution for the basic within-host organism HIV model ($f = f_1$). Parameters: $\delta = 5$ day^{-1} mm^{-3}, $\alpha = 0.03$ day^{-1}, $p = 3$ day^{-1}, $T_{max} = 1700$ mm^{-3}, $\beta = 0.2$ day^{-1}, $\gamma = 3.0$ day^{-1}, $k = 0.003$ mm ^{3} day^{-1}, and $N = 9$. T is the level of uninfected T cells; T^* is the level of productively infected T cells; and V is the level of free virus particles in the blood

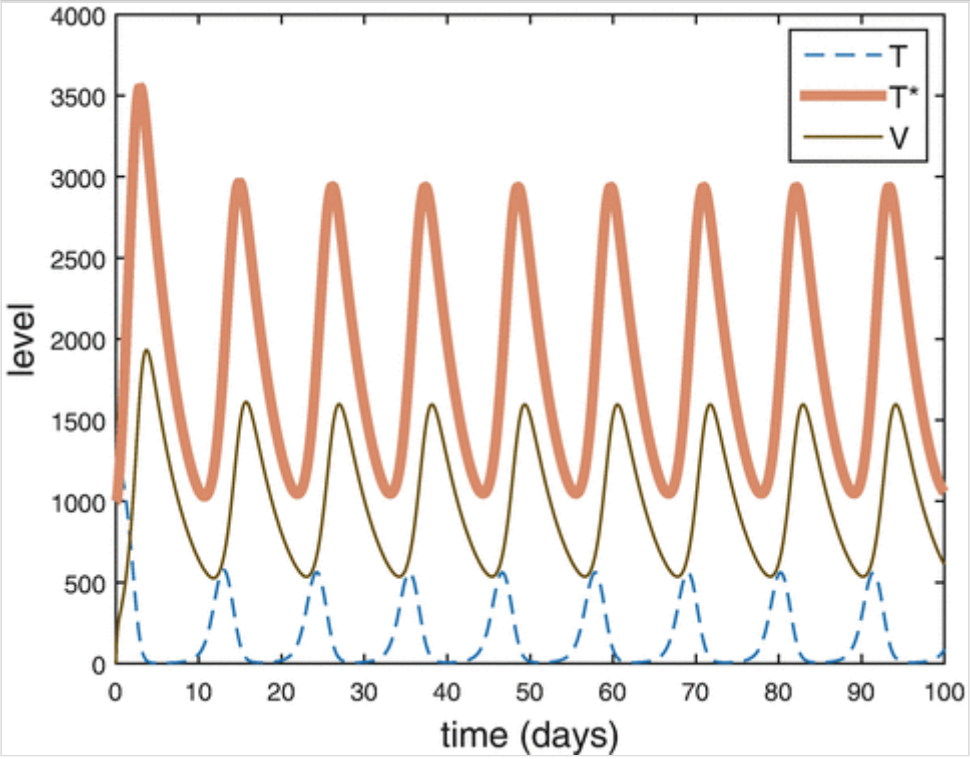

34.3.1. Comments on R_0

The above formula for R_0 is obtained following the procedure outlined in [59]. In fact, technically speaking that procedure would yield the square root of the expression given above. However, since R_0 is used to determine the local stability or instability of the disease-free steady state (stable if $R_0 < 1$ and unstable if $R_0 > 1$), it does not matter whether the square root is applied or not. Similar comments explain the difference between R_0 given above and the formula for R_0 given in [53]; the latter was derived before the now accepted procedure in [59] was known to the authors of [53].

34.4. Sustained Oscillations of the Within-Host Target Cell HIV Model: The Tat-Rev-Mediated Regulation of HIV-1 Replication

Here we review a mathematical model for Tat-Rev-mediated regulation of HIV-1 replication. This model was originally developed and used to examine the dynamics of the accumulation of Tat and Rev proteins and the viral RNA in an infected macrophage, that is, persistently producing the virus particles [17]. In this model, two specific hypotheses on the recycling (nuclear import/export cycle) of the HIV-1 Rev protein were considered. The first hypothesis is that Rev is released from the export complex and binds to importin-β in the cytoplasm [18]. The second hypothesis is that Rev returns into the nucleus directly at the nuclear pore complex without the export of Rev to the cytoplasm [60, 61]. The mathematical model was calibrated using published experimental data. It predicts the existence of oscillatory dynamics which depends on the efficacy of the interaction between the Tat protein and TAR and on the transport kinetics regulated by the Rev protein [17]. Below, we describe the formal representation of this model.

34.4.1. A Mathematical Model of the Tat-Rev-Mediated Regulation of HIV-1 Replication

The mathematical model of the Tat-Rev-mediated regulation of the intracellular HIV-1 replication is specified using the biochemical systems formalism [62]. Two elementary types of reactions, bimolecular and monomolecular, are considered. Below we discuss some standard notation to represent the chemical reactions. A bimolecular reaction can be formally presented as follows:

$$A + B \leftrightarrow C : k_1, k_2 \tag{34.4}$$

where A, B, and C are concentrations of reactants in the reaction; k_1 and k_2 are rate constants of the forward and reverse reactions, respectively. According to the law of mass action, the system of ordinary differential equations (ODEs) corresponding to bimolecular reaction (34.4) can be written as follows:

$$\frac{dA(t)}{dt} = \frac{dB(t)}{dt} = -\frac{dC(t)}{dt} = -k_1 A(t)B(t) + k_{12}C(t) \tag{34.5}$$

These equations describe the local rates of changes in concentrations of reactants A, B, and C in a fixed volume.

A monomolecular reaction can be formally presented as follows:

$$[a]\, A \rightarrow [b_1]\, B_1 + \cdots + [b_n]\, B_n : k \tag{34.6}$$

where A and B_i are concentrations of the reaction reactant and products, respectively; k is the reaction rate constant; a and b_i are the stoichiometric coefficients. The system of ordinary differential equations (ODEs) corresponding to monomolecular reaction (34.6) can be written as follows:

$$\frac{dA(t)}{dt} = -akA(t),\ \frac{dB_i(t)}{dt} = b_i kA(t), \quad i = 1, \ldots, n \tag{34.7}$$

The system (34.4) determines the local rates of changes in concentrations for reaction reactants in a fixed volume. To simplify the notation of monomolecular reactions, we will omit the stoichiometric coefficient of 1. The value of $a = 0$ corresponds to a reaction, where reactant A plays a role of an infinite resource for the reaction products.

34.4.2. Elementary Subsystems of the Tat-Rev Model

The mathematical model of a Tat-Rev-mediated regulatory network of HIV-1 replication consists of the following 14 elementary subsystems (Fig. 34.2):

1. The initiation of transcription from the HIV-1 proviral long terminal repeat (LTR) promoter, $\mathrm{LTRP_{HIV1}}$, leading to formation of the elongation complex $\mathrm{RNAPII_{TAR}}$ that is prone to termination at a TAR element is formally presented as follows:

$$[0]\,\mathrm{LTRP_{HIV1}} \rightarrow \mathrm{RNAPII_{TAR}} : k_{\mathrm{transcr,ini}}\mathrm{proV}$$

where $k_{\mathrm{transcr\,,\,ini}}$ is the rate constant of the transcription initiation, and proV is the number of proviral DNA genomes in the cell.

2. The passage of TAR element by RNA polymerase II (RNAPII). It is assumed that RNAPII is terminated at the TAR element and forms short RNAs *microRNA* with probability λ. Thus, the termination of RNAPII transcription at the TAR element is avoided, and the elongation complex $\mathrm{RNAPII_{DNAunit_1}}$ is formed with probability (1– λ). This process can be formally presented as follows:

$$\mathrm{RNAPII_{TAR}} \rightarrow [1-\lambda]\,\mathrm{RNAPII_{DNAunit_1}} + [\lambda]\,\mathrm{microRNA} : k_{\mathrm{delay}}$$

where k_{delay} is the rate constant for the RNAPII exit from the pausing site at the TAR element.

3. The Tat-dependent antitermination of transcription at the TAR element is described using the following two reactions:

$$\mathrm{RNAPII_{TAR}} + \mathrm{Tat_{nuc}} \leftrightarrow \mathrm{Tat_{TAR}} : k_{\mathrm{assoc,Tat_{TAR}}}, k_{\mathrm{dissoc,Tat_{TAR}}}$$

$$\mathrm{Tat_{TAR}} \rightarrow \mathrm{RNAPII_{DNAunit_1}} + \mathrm{Tat_{nuc}} : k_{\mathrm{antiterm}}$$

The first reaction describes the interaction of the complex $\mathrm{RNAPII_{TAR}}$ at the TAR element with the nuclear fraction of the Tat protein $\mathrm{Tat_{nuc}}$ resulting in the formation of a $\mathrm{Tat_{TAR}}$ complex. The second reaction describes Tat-dependent antitermination leading to the formation of the elongation complex, $\mathrm{RNAPII_{DNAunit_1}}$, and the release of the Tat protein. $k_{\mathrm{assoc},Tat_{TAR}}$ and $k_{\mathrm{dissoc},Tat_{TAR}}$ are the rate constants for the association and dissociation of Tat protein with the TAR element, respectively; k_{antiterm} is the rate constant of transcriptional antitermination by the Tat protein at the TAR element.

4. To model a delay in the synthesis of 9 kb RNAs, a chain of n_{DNAunit} reactions was introduced to formally present transcription elongation from the TAR element to the transcription terminator site. This process can be written as follows:

$$\mathrm{RNAPII_{DNAunit_i}} \rightarrow \mathrm{RNAPII_{DNAunit_{i+1}}} : k_{\mathrm{transcr,elong},i}, \quad i = 1, \ldots, n_{\mathrm{DNAunit}}$$

where $\mathrm{RNAPII_{DNAunit_i}}$ is the level of elongating complexes at the *i*-th segment of the proviral DNA; $k_{\mathrm{transcr\,,\,elong\,,\,}i}$ is the transcription elongation rate constant at the *i*-th segment. It is assumed that the lengths of the segments and the transcription rates are the same.

5. The transcription termination finalizing the elongation of the last (n_{DNAunit} +1)-th segment of the

proviral DNA and the release of the precursor molecule of the nuclear 9 kb RNA, pre9kbRNA$_{nuc}$, is formally presented as follows:

$$\mathrm{RNAPII}_{\mathrm{DNAunit}_{n_{\mathrm{DNAunit}}+1}} \rightarrow \mathrm{pre9kbRNA}_{\mathrm{nuc}} : k_{\mathrm{transcr,term}}$$

where $k_{\mathrm{transcr\ ,\ term}}$ is the transcription termination rate constant of the nuclear 9 kb RNA.

6. The maturation of the 9 kb mRNA primary transcript into the mature 9 kb mRNA form, 9kbRNA$_{nuc}$, is modeled as follows:

$$\mathrm{pre9kbRNA}_{\mathrm{nuc}} \rightarrow \mathrm{9kbRNA}_{\mathrm{nuc}} : k_{\mathrm{modif}}$$

where k_{modif} is the rate constant of the primary 9 kb RNA maturation process.

7. The splicing of the 9 kb RNA leading to the formation of 4 kb RNA, 4kbRNA$_{nuc}$, in the nucleus is represented by:

$$\mathrm{9kbRNA}_{\mathrm{nuc}} \rightarrow \mathrm{4kbRNA}_{\mathrm{nuc}} : k_{\mathrm{splicing,94}}$$

where $k_{\mathrm{splicing\ ,\ 94}}$ is the rate constant for the splicing of 9 kb to 4 kb mRNAs.

8. The alternative splicing of 9 kb and 4 kb RNAs to 2 kb mRNAs, which encode Tat, 2kbRNA$_{nuc}$, and Rev, 2kbRNA$_{nuc}$, proteins, is described as follows:

$$x\mathrm{kbRNA}_{\mathrm{nuc}} \rightarrow [\delta_{x,\mathrm{Tat}}]\, 2\mathrm{kbRNA}_{\mathrm{Tat,nuc}} + [\delta_{x,\mathrm{Rev}}]\, 2\mathrm{kbRNA}_{\mathrm{Rev,nuc}} : k_{\mathrm{splicing,x2}}, \quad x \in \{9, 4\}$$

where $k_{\mathrm{splicing\ ,\ x2}}$ is the rate constant for the splicing of 9 kb and 4 kb to 2 kb mRNAs; $\delta_{x\ ,\ \mathrm{Tat}}$ and $\delta_{x\ ,\ \mathrm{Rev}}$ are the fractions of 2 kb RNAs, 2kbRNA$_{\mathrm{Tat\ ,\ nuc}}$ and 2kbRNA$_{\mathrm{Rev\ ,\ nuc}}$, respectively, produced by the alternative splicing of 9 kb and 4 kb mRNAs.

9. The transport of 2 kb mRNAs into the cytoplasm is described as follows:

$$2\mathrm{kbRNA}_{\mathrm{X,nuc}} \rightarrow 2\mathrm{kbRNA}_{\mathrm{X,cyt}} : k_{\mathrm{transport,2kbRNA_X}}, \quad X \in \{\mathrm{Tat}, \mathrm{Rev}\}$$

where $2\mathrm{kbRNA}_{X,\ \mathrm{cyt}}$ is the concentration of 2 kb mRNAs encoding Tat and Rev in the cytoplasm; $k_{\mathrm{transport,2kbRNA}_X}$ is the rate constant of the nuclear export of 2 kb RNAs of the Tat and Rev proteins.

10. The synthesis of Tat and Rev proteins in the cytoplasm is described as a chain of reactions considering the initiation, elongation, and termination of the translation:

$$[0]\, 2\mathrm{kbRNA}_{X,\mathrm{cyt}} \rightarrow 2\mathrm{kbRNA}_{X,\mathrm{transl}_{,\mathrm{elong}_i}} : k_{\mathrm{transl,ini},X}$$

$$2\mathrm{kbRNA}_{X,\mathrm{transl}_{,\mathrm{elong}_i}} \rightarrow 2\mathrm{kbRNA}_{X,\mathrm{transl}_{,\mathrm{elong}_{i+1}}} : k_{\mathrm{transl,elong}_i}, \quad i = 1, \ldots, n_X,$$

$$2\text{kbRNA}_{X,\text{transl}_{,\text{elong}_{n_X+1}}} \rightarrow \text{prot}_{X,\text{cyt}} : k_{\text{transl,term},n_X+1}, \quad X \in \{\text{Tat}, \text{Rev}\}$$

where $k_{\text{transl , ini , }X}$ is the rate constant of translation initiation; $k_{\text{transl,elong}_i}$ is the rate constant of translation elongation for the *i*-th segment, and $k_{\text{transl,term},n_X+1}$ is the rate constant of translation termination for the (n_X+1)-th segment. The first reaction describes the initiation of the translation of Tat and Rev proteins in the cytoplasm resulting in the formation of the elongation complex $2\text{kbRNA}_{X,\text{transl}_{,\text{elong}_1}}$. The next n_X reactions describe the translation elongation for Tat and Rev proteins. The reaction chains were used to reproduce a delay in the synthesis of Tat and Rev. The set $2\text{kbRNA}_{X,\text{transl}_{,\text{elong}_i}}$ characterizes the number of elongation complexes on the *i*-th segment of the viral mRNAs. The last reaction describes the translation termination associated with the formation of Tat and Rev. $\text{prot}_{X\text{ , cyt}}$ denotes the amount of Tat and Rev proteins in the cytoplasm.

11. The transport of Tat and Rev proteins from the cytoplasm to the nucleus is modeled by the equation:

$$\text{prot}_{X,\text{cyt}} \rightarrow \text{prot}_{X,\text{nuc}} : k_{\text{transport,prot}_X}, X \in \{\text{Tat}, \text{Rev}\}$$

where $\text{prot}_{X\text{ , nuc}}$ is the abundance of Tat and Rev in the nucleus, and $k_{\text{transport,prot}_X}$ is the protein-specific rate constant for the transport of Tat and Rev from the cytoplasm to the nucleus.

12. The formation of the complexes of the Rev proteins with 9 kb and 4 kb RNAs is described as a sequence of n_{Rev} reactions resulting in the production of n_{Rev}-th complex. It is assumed that the complexes of Rev with 9 kb and 4 kb RNAs can take place both in the nucleus and the cytoplasm. The corresponding set of equations reads:

$$x\text{kbRNA}_y + \text{prot}_{\text{Rev}_y} \leftrightarrow \text{Rev}_1 x\text{kbRNA}_y : k_{\text{assoc,Rev}_1 X_y}, k_{\text{dissoc,Rev}_1 X_y}$$

$$\text{Rev}_i x\text{kbRNA}_y + \text{prot}_{\text{Rev}_y} \leftrightarrow \text{Rev}_{i+1} x\text{kbRNA}_y : k_{\text{assoc,Rev}_{i+1} X_y}, k_{\text{dissoc,Rev}_{i+1} X_y}$$

$$i = 1, \ldots, n_{\text{Rev}} - 1, x \in \{9, 4\}, y \in \{\text{nuc}, \text{cyt}\}$$

where $\text{Rev}_i x\text{kbRNA}_y$ is the level of complexes containing *i* molecules of the Rev proteins with either 4 kb or 9 kb RNAs in the nucleus or in the cytoplasm, respectively; $k_{\text{assoc,Rev}_{i+1} X_y}$ and $k_{\text{dissoc,Rev}_{i+1} X_y}$ are the association and dissociation rate constants, respectively, for the binding of Rev to 4 kb or 9 kb RNAs at the stage of the (*i* + 1)-meric complex formation in the nucleus or the cytoplasm.

13. The Rev-dependent transport of 9 kb and 4 kb RNAs from the nucleus ($\text{Rev}_i x\text{kbRNA}_{\text{nuc}}$) to the cytoplasm ($x\text{kbRNA}_{\text{cyt}}$) followed by the release of the Rev protein in the nucleus (at the nuclear pore) and in the cytoplasm is described as follows:

$$\text{Rev}_i x\text{kbRNA}_{\text{nuc}} \rightarrow x\text{kbRNA}_{\text{cyt}} + [\gamma_i] \text{prot}_{\text{Rev}_{\text{nuc}}} + [i - \gamma_i] \text{prot}_{\text{Rev}_{\text{cyt}}} : k_{\text{transport},X,i}$$

$$i = 1, \ldots, n_{\text{Rev},x} - 1, \quad x \in \{9, 4\}$$

where $k_{\text{transport , }X\text{ , }i}$ is the rate constant of the nuclear export of the *i*-meric complex of Rev with 9 kb or 4 kb RNAs; γ_i is the fraction of Rev proteins released from the *i*-meric complex at the nuclear pore; $(i - \gamma_i)$ is the fraction of Rev proteins released from the *i*-meric complex in the cytoplasm.

14. The degradation of the 9 kb, 4 kb, and 2 kb RNAs in the nucleus and the cytoplasm is described by the following first-order reactions:

$$x\text{kbRNA}_y \rightarrow \varnothing : k_{\text{degr},x\text{kbRNA}_y}$$

$$2\text{kbRNA}_y \rightarrow \varnothing : k_{\text{degr},2\text{kbRNA}_y}$$

$$\text{Rev}_i\, x\text{kbRNA}_y \rightarrow [\gamma_i]\, \text{prot}_{\text{Rev}_{\text{nuc}}} : k_{\text{degr},\text{Rev}_i x\text{kbRNA}_y}$$

$$\text{prot}_{X_y} \rightarrow \varnothing : k_{\text{degr},\text{prot}_{X_y}}$$

$$i = 1, \ldots, n_{\text{Rev},x} - 1, \quad x \in \{9, 4\}, X \in \{\text{Tat}, \text{Rev}\}, y \in \{\text{nuc}, \text{cyt}\}$$

where $k_{\text{degr},x\text{kbRNA}_y}$ is the 9 kb and 4 kb RNA degradation rate constants in the nucleus and the cytoplasm; $k_{\text{degr},prot_{X_y}}$ are rate constants of the specific degradation of the Tat and Rev proteins; and $k_{\text{degr},\text{Rev}_i x\text{kbRNA}_y}$ are degradation rate constants for 9 kb and 4 kb RNAs in the *i*-meric complex with the Rev protein in the nucleus and cytoplasm.

Model parameters were directly estimated from the published experimental data or indirectly from physical and chemical properties of the model processes and components (Table 34.1). Below we present some of those estimates.

Table 34.1

Model parameter used for numerical simulations of the Tat-Rev-mediated regulation of HIV-1 replication

Subsystem number	Parameter notation	Units	Reference value	Reference
1	$k_{\text{transcr , ini}}$	Transcription initiation/(min genome)	0.25 (for nonactivated cell)	[63, 64]
			25 (for activated cell)	
	$\text{LTRP}_{\text{HIV1}}$	Elements/nucleus	1	Assigned
2	k_{delay}	1/min	1	Assigned
	λ		0.99	Estimated
3	$k_{\text{assoc},Tat_{TAR}}$	Elements/(nucleus min)	0.0017	[65]
	$k_{\text{dissoc},Tat_{TAR}}$	1/min	1	
	k_{antiterm}	1/min	60	Assigned

Subsystem number	Parameter notation	Units	Reference value	Reference
4	$k_{\text{transcr , elong , } i}$, $i = 1$, … , n_{DNAunit}	1/min	5.33	Derived
	n_{DNAunit}	Dimensionless	20	Assigned
5	$k_{\text{transcr , term}}$	1/min	60	Assigned
6	k_{modif}	1/min	60	Assigned
7	$k_{\text{splicing , 94}}$	1/min	0.0415	[66, 67, 68]
8	$k_{\text{splicing , 42}}$	1/min	0.0415	
	$k_{\text{splicing , 92}}$	1/min	0.0207	Assigned
	$\delta_{9\text{ , Tat}}=\delta_{4\text{ , Tat}}$	Dimensionless	0.115	Estimated from [69]
	$\delta_{9\text{ , Rev}}=\delta_{4\text{ , Rev}}$	Dimensionless	0.115	
9	$k_{\text{transport,2kbRNA}_X}$, $X \in$ {Tat, Rev}	1/min	0.0767	[28]
10	$k_{\text{transl , ini , } X}$, $X \in$ {Tat, Rev}	1/min	10	Assigned
	$k_{\text{transl,elong}_i}, X \in \{\text{Tat}, \text{Rev}\}$	1/min	18	Derived
	$k_{\text{transl,term},n_X+1}$, $X \in$ {Tat, Rev}	1/min	60	Assigned
	n_X , $X \in$ {Tat, Rev}	Dimensionless	20	Assigned
11	$k_{\text{transport,prot}_X}, X \in \{\text{Tat}, \text{Rev}\}$	1/min	0.347	[70]
12	$k_{\text{assoc,Rev}_1X_{nuc}}$, $i = 1$, … , $n_{\text{Rev}} - 1$, $x \in$ {9, 4}	Copy/(nucleus min)	0.59	[29]
	$k_{\text{assoc,Rev}_1X_{cyt}}$, $i = 1$, … , $n_{\text{Rev}} - 1$, $x \in$ {9, 4}			
	$k_{\text{dissoc,Rev}_1X_{nuc}}$, $i = 1$, … , $n_{Rev} - 1$, $x \in$ {9, 4}	1/min	8.4	
	$k_{\text{dissoc,Rev}_1X_{cyt}}$, $i = 1$, … , $n_{\text{Rev}} - 1$, $x \in$ {9, 4}			
13	$k_{\text{transport , } x\text{ , 1}}$, $x \in$ {9, 4}	1/min	0	[71]
	$k_{\text{transport , } X\text{ , 1}}$, $i = 2$, … , $n_{\text{Rev , } x} - 1$, $x \in$ {9, 4}	1/min	0.0767	[28]
	γ_i , $i = 1$, … , $n_{\text{Rev , } X}$	Dimensionless	12	Quantified following the recycling in the nuclear pore hypothesis
12,13	$n_{\text{Rev , } x}$ $x \in$ {9, 4}	Dimensionless	12	[29, 72, 73]

Subsystem number	Parameter notation	Units	Reference value	Reference
14	$k_{\mathrm{degr},x\mathrm{kbRNA}_y}$, $X \in \{\mathrm{Tat}, \mathrm{Rev}\}$, $y \in \{\mathrm{nuc}, \mathrm{cyt}\}$	1/min	0.0029	[74]
	$k_{\mathrm{degr},2\mathrm{kbRNA}_y}, y \in \{\mathrm{nuc}, \mathrm{cyt}\}$			
	$k_{\mathrm{degr},\mathrm{Rev}_i x\mathrm{kbRNA}_y}$ $i = 1, \ldots, n_{\mathrm{Rev},x} - 1$, $x \in \{9, 4\}$, $y \in \{\mathrm{nuc}, \mathrm{cyt}\}$			
	$k_{\mathrm{degr},\mathrm{prot}_{X_{\mathrm{nuc}}}}, X \in \{\mathrm{Tat}, \mathrm{Rev}\}$	1/min	0.000722	[75]
	$k_{\mathrm{degr},\mathrm{prot}_{X_{\mathrm{cyt}}}}, X \in \{\mathrm{Tat}, \mathrm{Rev}\}$	1/min	0.00289	
Auxiliary parameters	$r_{\mathrm{transcr},\mathrm{elong}}$	Nucleotides/min	2400	[66, 76]
	$r_{\mathrm{transl},\mathrm{elong}}$	Nucleotides/min	1800	[77]
	$9\mathrm{kbRNA}_{\mathrm{nuc}}$	Nucl	9000	[19]
	$2kbRNA_{\mathrm{nuc}}$	Nucl	2000	
Modified from Likhoshvai et al. [17]				

Transcription

The transcription elongation rate in eukaryotic cells ranges from 25 to 60 nucleotides/s [66, 76, 78]. A similar estimate for HIV-1 (~33 nucleotides/s) was obtained using a reporter construct integrated at specific transcription site of the viral genome [79, 80]. The basal transcription rate starting from the HIV-1 promoter in nonactivated cells is assumed to be ~40 nucleotides/s, whereas transcription initiation is assumed to be ~0.25 events/min.

The exit rate of RNAPII from the transcription elongation pausing state is formally quantified by the parameter k_{delay}. The value of this parameter is estimated to be 1/min assuming that the duration of pausing is ~1 min. Pausing time is assumed to be longer than the time of the transcription through the TAR element by RNAPII without pausing, which ranges from 1 to 2 s. The later estimate results from the base length of the TAR element being 59 nucleotides and an elongation rate of about 25–60 bases/s [66, 76]. In the absence of Tat protein, RNAPII located at the TAR element can spontaneously leave the pausing site and either continue the transcription or terminate it. We assumed that in the absence of Tat, the pausing leads to transcription termination for about 99 out of 100 RNAPII molecules. RNAPII can also exit the pausing site and continue the transcription in the presence of Tat protein due to its interaction with the secondary structure of the TAR element on synthesized RNA. The availability of Tat in the nucleus activates the synthesis of 9 kb RNA by up to 100-fold [23, 24, 25].

The antitermination efficacy in the model is described by the parameter k_{antiterm}. This parameter is estimated to be 60 min^{-1}. Parameters $k_{\mathrm{assoc},Tat_{TAR}}$ and $k_{\mathrm{dissoc},Tat_{TAR}}$ represent the association and dissociation rate constants, respectively, for Tat protein with the secondary structure of the partially synthesized RNA at the TAR element region (see Table 34.1). The published data provide an estimate for the ratio $K_{d,\mathrm{Tat}} = k_{\mathrm{dissoc},\mathrm{Tat}_{\mathrm{TAR}}} / k_{\mathrm{assoc},\mathrm{Tat}_{\mathrm{TAR}}}$ with a range of 100–400/μM [65, 81]. The dissociation rate constant is

assumed to be $k_{\mathrm{dissoc},Tat_{TAR}}$ =1/min. It was derived using a value of $K_{d\ ,\mathrm{Tat}}$=100/μM with the volume of the nucleus set to 100 μm^3.

Splicing

The characteristic time of splicing the pre-mRNAs during transcription is about 5–10 min and does not depend on intron size [66, 67, 68].

Transport

The transport of 2 kb mRNA from the nucleus to the cytoplasm is carried out by endogenous cellular mechanisms. Active transport through the nuclear pore is a relatively fast process (10–100 molecules per the pore per second) [82, 83]. It is formally described in the model as a monomolecular reaction. The transport of 9 kb and 4 kb RNAs out of the nucleus is mediated by a Rev-dependent mechanism. The binding of Rev protein to the RRE site of the intron-containing HIV-1 mRNA takes place sequentially, and the assembled oligomeric complex, Rev/RRE, can contain up to 12 molecules of Rev protein [29, 72, 73]. The transport of Tat and Rev back to the nucleus is mediated by endogenous cellular mechanisms, i.e., a nuclear localization sequence (NLS) signal. The transport kinetics of Tat was experimentally measured, and the specific rate constant of nuclear import is ~0.3 min^{-1} [70]. Here, Tat and Rev nuclear import rate constants are set to 0.347 min^{-1}.

Translation

The average ribosome density per codon in eukaryotic cells is 0.017 [77, 84]. Taking into account a length of Tat/Rev mRNA of about 2000 bases, the number of available ribosomes at this segment can be estimated to be ~11. The translation elongation rate of mRNA depends on the initiation rate, and the initiation rate in the model is assumed to be ~10 events/min. Thus, the translation elongation rate constant is ~30 nucleotides/s.

mRNA Stability

The stability of HIV-1 mRNA in the nucleus and the cytoplasm is about the same [85] with a half-life for Tat mRNA ranging from 4 to 5 h and for Rev mRNA from 4 to 13 h [74, 86].

Stability of Proteins

The half-life of Rev is assumed in the model to be 4 h in the cytoplasm and 16 h in the nucleus [75].

The parameters of the mathematical model of the Tat-Rev-mediated regulation of HIV-1 replication used for numerical simulations are presented in Table 34.1.

The overall rate of change for every model variable is calculated by adding or subtracting the rates of the elementary subsystems where the current variable is produced or consumed, respectively. The initial value problem for the model equations was solved numerically using Gear's method based on backward differentiation formulas [87] implemented in Fortran [17]. The model with parameter values presented in Table 34.1 predicts sustained oscillations of HIV components in the within-host target cell system controlled by the Tat-Rev regulatory circuit (Fig. 34.5).

Fig. 34.5

Kinetics of the viral RNA and proteins synthesized in an activated cell with one provirus copy. (**a**) The abundance of free Tat molecules (not bound to RNA at the TAR element) and Rev molecules (not bound to 9 kb RNA and 4 kb RNA) in the nucleus. (**b**) The abundance of free Tat and Rev proteins in the cytoplasm (their kinetics is identical as the corresponding model parameters for these two proteins are identical, and the

nuclear export of Rev to the cytoplasm is not considered). (**c**) The abundance of 2 kb RNA molecules in the nucleus and cytoplasm encoding the Tat and Rev proteins

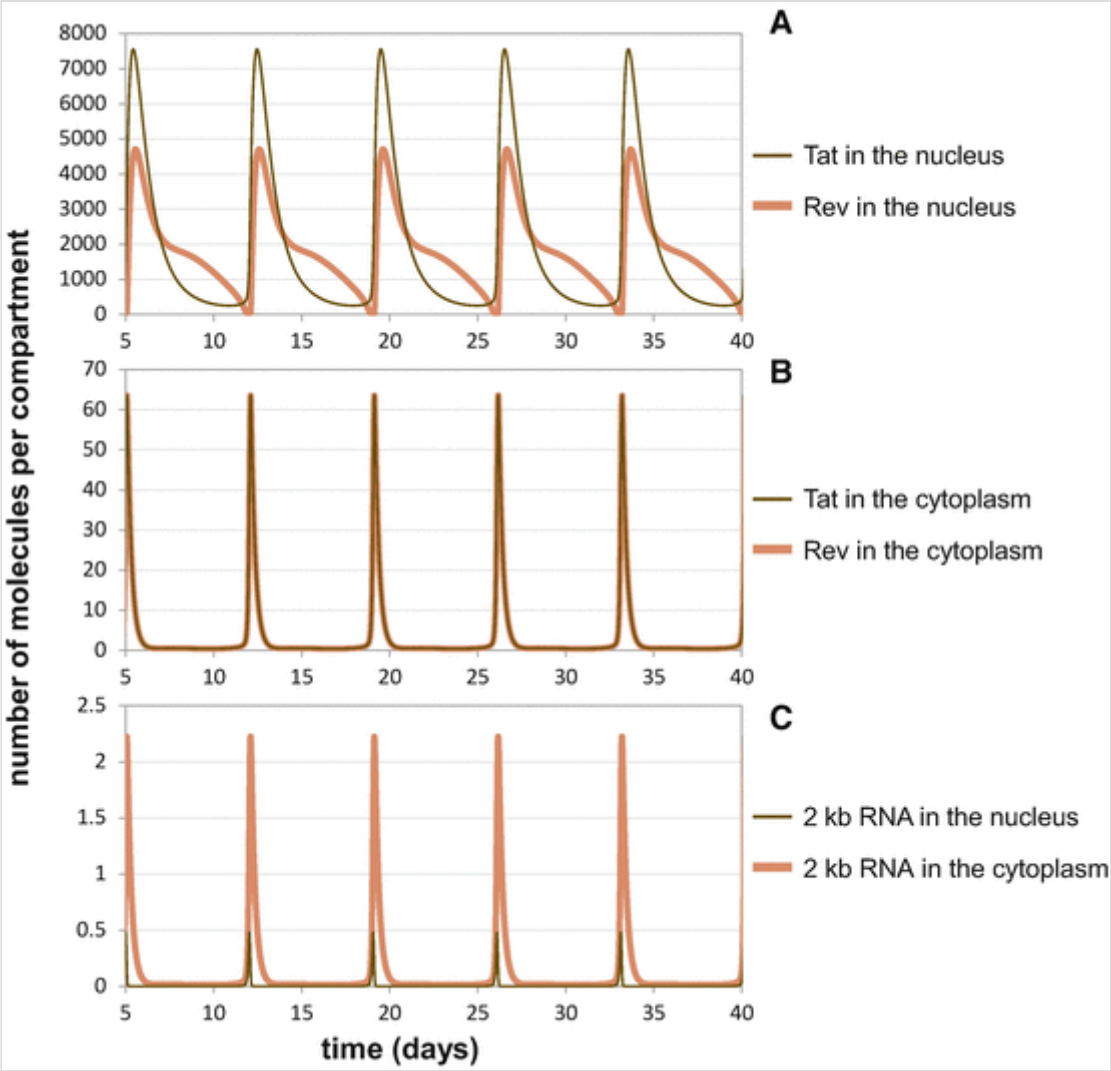

It should be noted that the oscillatory pattern in Fig. 34.5 appears as a limit cycle. The period of the cycle is rather long, being more than 150 h. The amplitude of oscillations in the concentrations of Tat and Rev proteins and the 2 kb RNAs encoding Tat and Rev over one period is quite significant. The simulations further predict that the 2 kb RNA molecules are present in trace amounts and are amenable to detection during a rather short-time window of about 10 h as compared to the cycle period. The above solutions were computed under the assumption that Rev-regulated export of 9 kb RNA and 4 kb RNA from the nucleus to the cytoplasm does not lead to the exit of Rev protein from the nucleus to the cytoplasm, which is in agreement with the hypothesis of Rev recycling at the nuclear pore [60]. The formation of complexes of the de novo synthesized Rev proteins with the 9 kb RNA and 4 kb RNA molecules in the cytoplasm compartment was not considered.

34.5. Parameter Sensitivity Analysis for Periodic Solutions for the Basic Within-Host Organism and Within-Host Target Cell HIV Models

Theoretical analysis of the basic within-host organism model [53] and the parameter sensitivity analysis of the basic within-host target cell HIV model reveal that both models have oscillatory dynamics within a wide range of parameters. For example, the basic within-host organism model has periodic solutions within a wide range of

death rates for the uninfected target cells (Fig. 34.6). For certain parameter sets, this model exhibits oscillatory dynamics with half-lives of the uninfected target cells varying from less than a day to more than 100 days. This range of half-lives covers different groups of potential target cells, including short-lived (e.g., T cells) and long-lived (e.g., macrophages) ones. Similarly, the basic within-host target cell model has periodic solutions within a wide range of half-life times for Tat and Rev proteins (Fig. 34.7). This model can oscillate with half-lives of Tat and Rev proteins in the nucleus and the cytoplasm varying from a few hours to a few hundred hours. The period and amplitude of oscillations can be different for different half-lives of the viral regulatory proteins. The kinetic properties and potential oscillatory dynamics of the basic within-host target cell model were previously systematically investigated [17]. Particularly, it was shown that this model has robust oscillatory dynamics for wide ranges of kinetic parameters of such processes and quantities as: (1) The nuclear export of the HIV-1 Rev protein to the cytoplasm; (2) The variation of provirus copy numbers; (3) The abundance of Rev protein in the complexes with 9 kb RNA and 4 kb RNA; (4) The transcription antitermination at the TAR element; (5) The oligomerization of Rev protein and the complex transport; (6) The 2 kb RNA translation initiation efficacy; (7) The Rev-mRNA stability

Fig. 34.6

Parameter sensitivity analysis for periodic solutions for the basic within-host organism HIV model ($f = f_1$). Parameter α was varied between 0.01 and 1 day^{-1}. Other parameters were fixed as follows: $\delta = 10$ day^{-1} mm^{-3}, $p = 3$ day^{-1}, $T_{max} = 1500$ mm^{-3}, $\beta = 0.24$ day^{-1}, $\gamma = 2.4$ day^{-1}, $k = 0.0027$ mm ^{3} day^{-1}, and $N = 10$. T is the level of uninfected T cells; T^* is the level of productively infected T cells; and V is the level of free virus particles in the blood

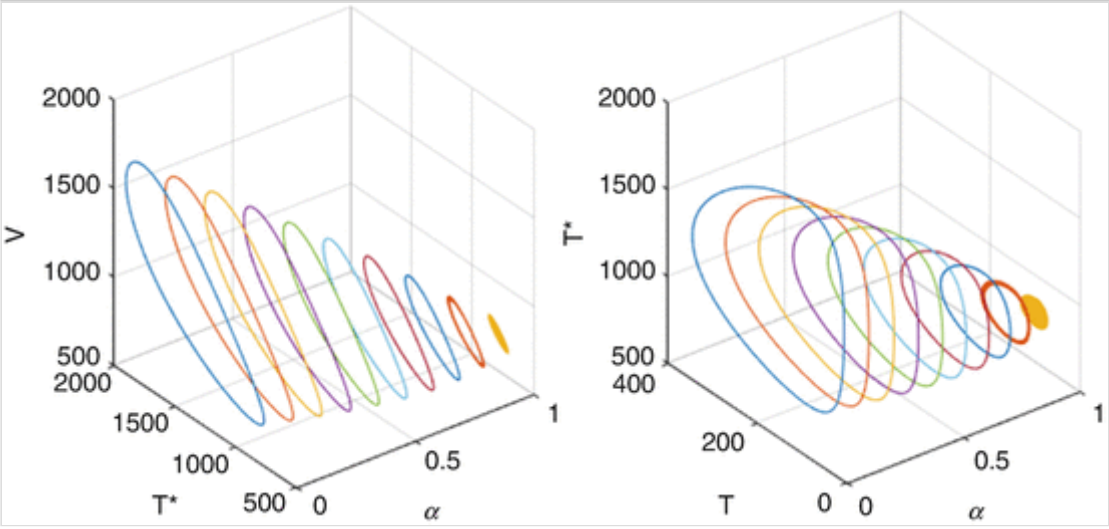

Fig. 34.7

Parameter sensitivity analysis for periodic solutions for the basic within-host target cell HIV model. Half-life time ($\tau_{1/2}$) of Tat and Rev in the nucleus and the cytoplasm were varied. (**a**) $\tau_{1/2} = 2.6$ h for Tat and Rev both in the nucleus and the cytoplasm. (**b**) $\tau_{1/2} = 3.2$ h for Tat and Rev both in the nucleus and the cytoplasm. (**c**) $\tau_{1/2} = 104$ h for Tat and Rev both in the nucleus and the cytoplasm. (**d**) $\tau_{1/2} = 208$ h for Tat and Rev both in the nucleus and the cytoplasm. $\gamma_i = 0$. Other parameters of the model used for these numerical simulations are presented in Table 34.1

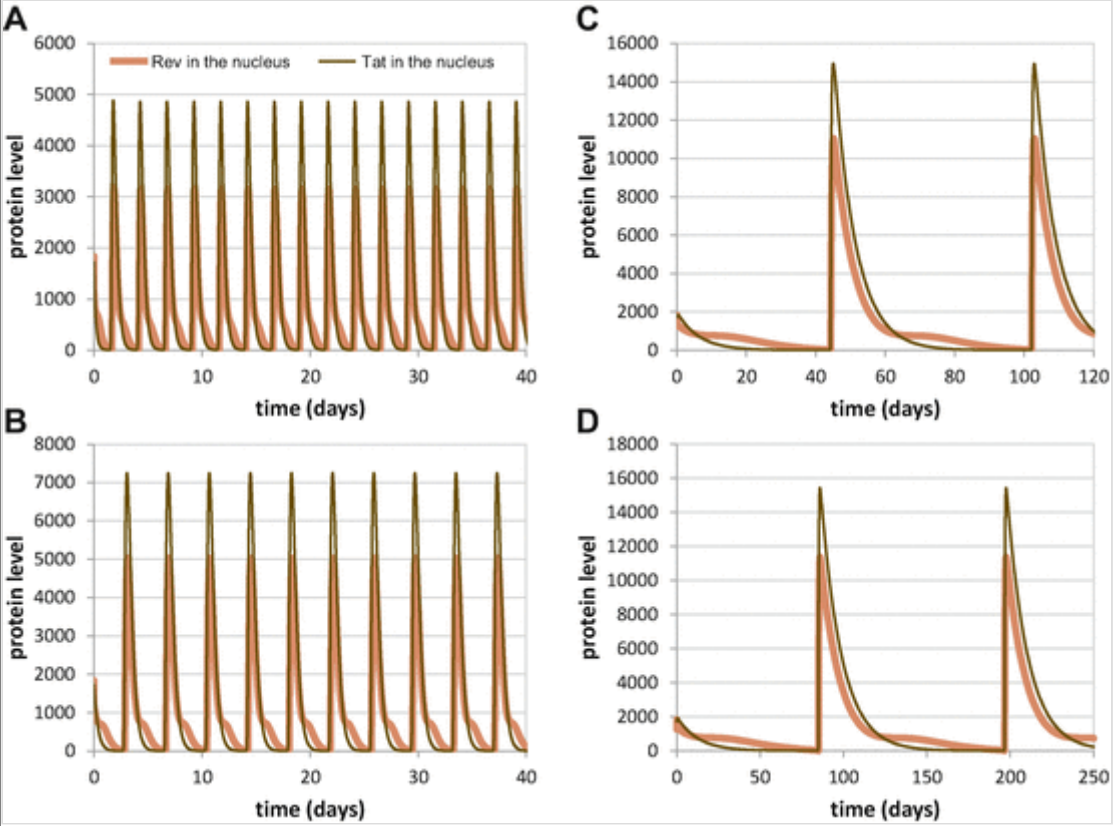

For example, the antitermination of transcription in the proposed model [17] is characterized by four parameters: the rate constant for the exit of RNAPII from the pausing site at TAR element (k_{delay}), the rate constant of the antitermination efficacy (k_{antiterm}), the forward, and the reverse rate constants of Tat protein binding to the secondary structure at the TAR element ($k_{\text{assoc},Tat_{TAR}}$ and $k_{\text{dissoc},Tat_{TAR}}$) (see Table 34.1). The ratio $K_{d\ ,\text{Tat}} = k_{\text{dissoc},Tat_{TAR}} / k_{\text{assoc},Tat_{TAR}}$ was experimentally estimated as 10 nM [19]. In order to characterize the impact of these parameters on transcription antitermination at the TAR element and the overall model dynamics, the ratio $K_{d\ ,\text{Tat}}$ and other two parameters (k_{delay} and k_{antiterm}) were varied as follows: k_{delay} = 0.25–10 min^{-1}, $k_{\text{antiterm}}/k_{\text{delay}}$ = 1–60, $k_{\text{dissoc},Tat_{TAR}}$ = 0.05–32 min^{-1}. Table 34.2 summarizes the results of parameter sensitivity analysis on the impact of Tat-dependent antitermination efficiency on the kinetics of the synthesis of viral components in the activated cell. The simulations were performed for a single virus genome copy since the calculations for higher copy numbers are not fundamentally different.

Table 34.2

The impact of the Tat-dependent antitermination efficiency on the kinetics of the synthesis of viral components in the activated cell

Constant of the delay of RNA polymerase II on TAR element k_{delay} (min^{-1})	**Regimes of the system functioning for different values of the dissociation constant of Tat-TAR complex $k_{\text{dissoc},Tat_{TAR}}$ (min^{-1})**									
	32	**16**	**8**	**4**	**2**	**1**	**0.5**	**0.25**	**0.1**	**0.05**
10	o[a]/o[b]/s[c]	o/o/o	o/o/o	o/o/o	o/o/o	s/s/s	s/s/s	s/s/s	s/s/s	s/s/s
4	o/s/s	o/s/s	o/s/s	o/o/o	o/o/o	o/o/o	s/s/s	s/s/s	s/s/s	s/s/s
1	o/s/s	o/s/s	o/s/s	o/s/s	o/s/s	o/o/o	o/o/o	o/o/o	s/s/s	s/s/s
0.25	o/s/s	o/s/s	o/s/s	o/s/s	o/s/s	o/s/s	o/s/s	o/o/o	o/o/o	s/o/o

Constant of the delay of RNA polymerase II on TAR element k (min)	Regimes of the system functioning for different values of the dissociation constant of Tat-TAR complex (min)									
	32	16	8	4	2	1	0.5	0.25	0.1	0.05

Note: *o* stands for oscillation; *s* stands for steady state

[a]The value of the antitermination efficiency constant $k_{\text{antiterm}} = k_{\text{delay}}$

[b]$k_{\text{antiterm}} = 10*k_{\text{delay}}$

[c]$k_{\text{antiterm}} = 60*k_{\text{delay}}$

AQ2

These computational results suggest the following:

1. The parameter space region corresponding to the oscillatory dynamics is rather large.

2. The parameters are not independent with respect to their impact on the HIV-1 replication system behavior. For example, for a decreased value of the pausing delay of RNAPII at the TAR element, the oscillatory dynamics is observed at higher values of the dissociation of the Tat-TAR complex. The oscillatory regime is shifted from the higher to lower values of $k_{\text{dissoc},Tat_{TAR}}$ with the increase of k_{delay} (see Table 34.2).

3. An increase in the proviral copy number extends the parameter region, for which the model has oscillatory dynamics of the viral proteins (the data are not shown).

4. The considered parameter values are in the physiological range and may well belong to the oscillatory domains of the model parameter space.

Thus, the analysis of both the within-host organism model and the within-host target cell HIV models revealed their high potential to generate oscillatory dynamics. In the case of the basic within-host organism HIV model, the virus persists in the host and the model solutions approaching either a chronic disease steady state or a periodic orbit if the basic reproduction number $R_0 > 1$. If $R_0 < 1$, then the virus is cleared and the disease dies out [53]. In the case of the basic within-host target cell HIV system, the oscillatory dynamics of the model essentially depends on a Rev protein shuttling mechanism, the stability of the Rev mRNA, and the interaction parameters of Rev protein with the RRE site on the intron-containing RNA [17].

Taking into account that the parametric domain corresponding to the oscillatory mode of HIV-1 replication is quite large, we hypothesize that the predicted phenomenon is not just a modeling artifact but may take place under certain conditions in an infected target cell or in a host cell population. One of the indirect indications in favor of this hypothesis is the ability of HIV-1 to establish a long-term persistent production of the infectious particles in humans [88]. We speculate that the identified oscillatory dynamics of HIV-1 replication at both the intracellular level and at the level of cell populations can be one of the possible mechanisms for the maintenance of the prolonged within-host organism or within-host target cell virus persistence.

34.6. Discussion

Mathematical modeling of within-host pathogen dynamics has flourished over the past few decades [89]. These models have been used to describe the dynamics of various infectious diseases, such as HIV [7, 17, 90, 91], HCV [92, 93], HTLV [94, 95], IAV [96, 97, 98], HDV [99], HSV [100], CMV [101] as well as tuberculosis

[102, 103] and malaria [104, 105] infections. Testing specific hypotheses based on clinical data is often difficult since samples cannot always be frequently taken from patients and because techniques for detecting the pathogen may not be accurate. This only amplifies the importance of mathematical models in this area of research.

In this chapter we summarized several theoretical studies on the potential for oscillatory behavior of HIV infection at molecular and cellular levels. These studies emphasize some aspects of nonlinear and inherently multiscale properties of the host-virus system. These properties of the virus, along with others, such as rapid mutation, hiding viral surface components from neutralizing antibodies, proviral latency, removal of cell-surface receptors, and destruction of immune effectors [3], may potentially be the result of coevolution with the host immune system. These properties may also constantly drive and shape the ability of the virus to avoid immune eradication.

Consider the oscillatory behavior of the viral components from the viewpoint of a biological advantage. In our discussion, we will assume the broadly accepted paradigm stating that if a specific feature of a biological system stably persists through many generations, then this feature provides a certain evolutionary advantage in the struggle for survival. Now, the question is what type of benefit would the cycling dynamics of viral components production give to the virus as compared to a steady state one? In our view, the real advantage is that the likelihood of the survival of the HIV-1-infected cell population should increase.

Consider the population of infected macrophages bearing the provirus in a latent form. When these cells activate, viral RNAs and proteins will be synthesized, and virus particles will be assembled and bud from infected cells. These cells become a target for the immune system, with the likelihood of the cell to be recognized by cytotoxic T lymphocytes (CTLs) being proportional to the concentration of the virus-specific antigens that are expressed on the cell surface by major histocompatibility complex (MHC) class I molecules. It is clear that in the absence of specific hiding mechanisms, the probability of the infected cell being recognized and destroyed will increase as the viral replication rate increases. Therefore, after some time most of the infected cells would become highly vulnerable to immune system, probably leading to a complete elimination of the infected cell population.

If we assume that the HIV-1 life cycle follows an oscillatory behavior, virus production by every infected cell will cycle and, unless there is a synchronization mechanism, the infected cell population will cycle asynchronously. This implies that at any given time, only a fraction of infected cells will be actively producing virus, with the rest of them staying in a silent mode of viral replication. Obviously, the cells characterized by a low-level viral replication will be less recognizable for the immune system as compared to the active producers. Thus, the immune system will recognize and destroy only a fraction of infected cells at any given time. Therefore, the oscillatory dynamics of viral ontogenesis should increase the survival of the virus under the selection pressure of the immune system.

An additional mechanism contributing to long-term viral persistence in an infected cell may be linked to oscillations in the level of the viral regulatory protein Nef. It has been shown that Nef induces a reduction of MHC class I molecules at the cell surface via endocytosis [106, 107]. This in turn reduces the efficacy of the recognition and killing of infected cells by CTLs leading to a latent infection characterized by long-term low levels of viral replication.

There are additional advantages to a virus exhibiting an oscillatory phenotype, including another phenomenon that we call the “recovery effect.” Active viral production by the infected cell over a long period can lead to the exhaustion of its resources and, finally, to death. Therefore, the alternating phases of high- and low-level virus replication should allow the cell to replenish consumed resources and avoid dying. Thus, the recovery effect should increase virus survival and grant an evolutionary advantage.

Therefore, oscillatory dynamics of the viral components at both molecular and cellular levels can provide evolutionary advantages enabling the survival of a fraction of the infected target cells even under constant

pressure by the host immune system. This type of ontogenesis dynamics, independent of other specific protection mechanisms evolved by the virus, can contribute to long-term persistent production of the virus in humans, a remarkable emergent property of HIV.

34.7. Conclusions

Theoretically predicted oscillatory behaviors of the virus at both within-host organism and within-host target cell levels necessitates the development of multiscale models that integrate intracellular and cell population host-viral dynamical systems [91, 108]. These models will allow a systematic exploration of potential host-virus system oscillations and/or pulsatile and bursting behaviors of the virus at different scales, their potential interference or amplification, heterogeneity of the virus behavior within different target cell types (e.g., T cells or macrophages) or target cell subpopulations, and stochastic properties of the multiscale interaction between virus and the host immune system. Multiscale mathematical modeling of the within-host HIV dynamical system combined with relevant experimental measurements at cell population and single-cell [109] levels, especially with the ever improving super-resolution fluorescence microscopy [110, 111, 112], promises to facilitate the comprehensive understanding of this complex host-virus system and develop rational interventions into disease processes.

Acknowledgments

We thank Fred D. Mast, Samuel A. Danziger, and John D. Aitchison for critical reading of the manuscript and for discussion. AVR is supported by the National Institutes of Health (P41GM109824 and P50 GM076547). PDL is supported by the National Science Foundation (DMS grant 1411853). SIB is supported by the Russian Foundation for Basic Research (Grant 14-04-91164). GAB is supported by the Russian Foundation for Basic Research (Grant 14-01-00477) and the Russian Science Foundation (Grant 15-11-00029). TMK and VAL are supported by Russian Foundation for Basic Research (Grant No 16-01-00237a) and Budget Project (No 0324-2016-0008).

References

AQ3

1. Coffin JM (1995) HIV population dynamics in vivo: implications for genetic variation, pathogenesis, and therapy. Science 267(5197):483–489

2. Sloot PMA, Coveney PV, Ertaylan G, Müller V, Boucher CA, Bubak M (2009) HIV decision support: from molecule to man. Philos Transact A Math Phys Eng Sci 367(1898):2691–2703

3. Peterlin BM, Trono D (2003) Hide, shield and strike back: how HIV-infected cells avoid immune eradication. Nat Rev Immunol 3(2):97–107

4. Gougeon M-L (2003) Apoptosis as an HIV strategy to escape immune attack. Nat Rev Immunol 3(5):392–404

5. Malim MH, Emerman M (2008) HIV-1 accessory proteins – ensuring viral survival in a hostile environment. Cell Host Microbe 3(6):388–398

6. Appay V, Sauce D (2008) Immune activation and inflammation in HIV-1 infection: causes and consequences. J Pathol 214(2):231–241

7. Perelson AS, Ribeiro RM (2013) Modeling the within-host dynamics of HIV infection. BMC Biol 11:96

8. Perelson AS (2002) Modelling viral and immune system dynamics. Nat Rev Immunol 2(1):28–36

9. Perelson AS, Neumann AU, Markowitz M, Leonard JM, Ho DD (1996) HIV-1 dynamics in vivo: virion clearance rate, infected cell life-span, and viral generation time. Science 271(5255):1582–1586

10. Bonhoeffer S, May RM, Shaw GM, Nowak MA (1997) Virus dynamics and drug therapy. Proc Natl Acad Sci U S A 94(13):6971–6976

11. Ribeiro RM, Bonhoeffer S (2000) Production of resistant HIV mutants during antiretroviral therapy. Proc Natl Acad Sci U S A 97(14):7681–7686

12. Hammond BJ (1993) Quantitative study of the control of HIV-1 gene expression. J Theor Biol 163(2):199–221

13. Reddy B, Yin J (1999) Quantitative intracellular kinetics of HIV type 1. AIDS Res Hum Retrovir 15(3):273–283

14. Kim H, Yin J (2005) Robust growth of human immunodeficiency virus type 1 (HIV-1). Biophys J 89(4):2210–2221

15. Tameru B, Habtemariam T, Nganwa D, Ayanwale L, Beyene G, Robnett V, Wilson W (2008) Computational modelling of intracellular viral kinetics and CD4+ cellular population dynamics of HIV/AIDS. Adv Syst Sci Appl 8(1):40–45

16. Zarrabi N, Mancini E, Tay J, Shahand S, Sloot PMA (2010) Modeling HIV-1 intracellular replication: two simulation approaches. Procedia Comput Sci 1(1):555–564

17. Likhoshvai VA, Khlebodarova TM, Bazhan SI, Gainova IA, Chereshnev VA, Bocharov GA (2014) Mathematical model of the tat-rev regulation of HIV-1 replication in an activated cell predicts the existence of oscillatory dynamics in the synthesis of viral components. BMC Genomics 15(Suppl 12):S1

18. Karn J, Stoltzfus CM (2012) Transcriptional and posttranscriptional regulation of HIV-1 gene expression. Cold Spring Harb Perspect Med 2(2):a006916

19. Purcell DF, Martin MA (1993) Alternative splicing of human immunodeficiency virus type 1 mRNA modulates viral protein expression, replication, and infectivity. J Virol 67(11):6365–6378

20. Laspia MF, Rice AP, Mathews MB (1989) HIV-1 tat protein increases transcriptional initiation and stabilizes elongation. Cell 59(2):283–292

21. Marciniak RA, Calnan BJ, Frankel AD, Sharp PA (1990) HIV-1 tat protein trans-activates transcription in vitro. Cell 63(4):791–802

22. Feinberg MB, Baltimore D, Frankel AD (1991) The role of tat in the human immunodeficiency virus life cycle indicates a primary effect on transcriptional elongation. Proc Natl Acad Sci U S A 88(9):4045–4049

23. Bohan CA, Kashanchi F, Ensoli B, Buonaguro L, Boris-Lawrie KA, Brady JN (1992) Analysis of tat transactivation of human immunodeficiency virus transcription in vitro. Gene Expr 2(4):391–407

24. Graeble MA, Churcher MJ, Lowe AD, Gait MJ, Karn J (1993) Human immunodeficiency virus type 1 transactivator protein, tat, stimulates transcriptional read-through of distal terminator sequences in vitro.

Proc Natl Acad Sci U S A 90(13):6184–6188

25. Harrich D, Hsu C, Race E, Gaynor RB (1994) Differential growth kinetics are exhibited by human immunodeficiency virus type 1 TAR mutants. J Virol 68(9):5899–5910

26. Chojnacki J, Müller B (2013) Investigation of HIV-1 assembly and release using modern fluorescence imaging techniques. Traffic Cph Den 14(1):15–24

27. Richard N, Iacampo S, Cochrane A (1994) HIV-1 rev is capable of shuttling between the nucleus and cytoplasm. Virology 204(1):123–131

28. Love DC, Sweitzer TD, Hanover JA (1998) Reconstitution of HIV-1 rev nuclear export: independent requirements for nuclear import and export. Proc Natl Acad Sci U S A 95(18):10608–10613

29. Pond SJK, Ridgeway WK, Robertson R, Wang J, Millar DP (2009) HIV-1 rev protein assembles on viral RNA one molecule at a time. Proc Natl Acad Sci U S A 106(5):1404–1408

30. Felber BK, Drysdale CM, Pavlakis GN (1990) Feedback regulation of human immunodeficiency virus type 1 expression by the rev protein. J Virol 64(8):3734–3741

31. Weinberger LS, Dar RD, Simpson ML (2008) Transient-mediated fate determination in a transcriptional circuit of HIV. Nat Genet 40(4):466–470

32. Hong H-W, Lee S-W, Myung H (2013) Induced degradation of Tat by nucleocapsid (NC) via the proteasome pathway and its effect on HIV transcription. Virus 5(4):1143–1152

33. Jablonski JA, Amelio AL, Giacca M, Caputi M (2010) The transcriptional transactivator tat selectively regulates viral splicing. Nucleic Acids Res 38(4):1249–1260

34. Lata S, Ali A, Sood V, Raja R, Banerjea AC (2015) HIV-1 Rev downregulates Tat expression and viral replication via modulation of NAD(P)H:quinine oxidoreductase 1 (NQO1). Nat Commun 6:7244

35. Barkai N, Leibler S (2000) Circadian clocks limited by noise. Nature 403(6767):267–268

36. Hasty J, Dolnik M, Rottschäfer V, Collins JJ (2002) Synthetic gene network for entraining and amplifying cellular oscillations. Phys Rev Lett 88(14):148101

37. Leite MCA, Wang Y (2010) Multistability, oscillations and bifurcations in feedback loops. Math Biosci Eng MBE 7(1):83–97

38. Stricker J, Cookson S, Bennett MR, Mather WH, Tsimring LS, Hasty J (2008) A fast, robust and tunable synthetic gene oscillator. Nature 456(7221):516–519

39. Cao Y, Wang H, Ouyang Q, Tu Y (2015) The free energy cost of accurate biochemical oscillations. Nat Phys 11(9):772–778

40. Leloup J-C, Goldbeter A (2003) Toward a detailed computational model for the mammalian circadian clock. Proc Natl Acad Sci U S A 100(12):7051–7056

41. Hayot F, Jayaprakash C (2006) NF-kappaB oscillations and cell-to-cell variability. J Theor Biol 240(4):583–591

42. Krishna S, Jensen MH, Sneppen K (2006) Minimal model of spiky oscillations in NF-kappaB signaling. Proc Natl Acad Sci U S A 103(29):10840–10845

43. Pigolotti S, Krishna S, Jensen MH (2007) Oscillation patterns in negative feedback loops. Proc Natl Acad Sci U S A 104(16):6533–6537

44. Jensen PB, Pedersen L, Krishna S, Jensen MH (2010) A Wnt oscillator model for somitogenesis. Biophys J 98(6):943–950

45. Hoffmann A, Levchenko A, Scott ML, Baltimore D (2002) The IkappaB-NF-kappaB signaling module: temporal control and selective gene activation. Science 298(5596):1241–1245

46. Nelson DE, Ihekwaba AEC, Elliott M, Johnson JR, Gibney CA, Foreman BE, Nelson G, See V, Horton CA, Spiller DG, Edwards SW, McDowell HP, Unitt JF, Sullivan E, Grimley R, Benson N, Broomhead D, Kell DB, White MRH (2004) Oscillations in NF-kappaB signaling control the dynamics of gene expression. Science 306(5696):704–708

47. Wang Y, Paszek P, Horton CA, Kell DB, White MR, Broomhead DS, Muldoon MR (2011) Interactions among oscillatory pathways in NF-kappa B signaling. BMC Syst Biol 5:23

48. Hirata H, Yoshiura S, Ohtsuka T, Bessho Y, Harada T, Yoshikawa K, Kageyama R (2002) Oscillatory expression of the bHLH factor Hes1 regulated by a negative feedback loop. Science 298(5594):840–843

49. Kageyama R, Yoshiura S, Masamizu Y, Niwa Y (2007) Ultradian oscillators in somite segmentation and other biological events. Cold Spring Harb Symp Quant Biol 72:451–457

50. Bose I, Ghosh B (2007) The p53-MDM2 network: from oscillations to apoptosis. J Biosci 32(5):991–997

51. Perelson A, Nelson P (1999) Mathematical analysis of HIV-1 dynamics in vivo. SIAM Rev 41(1):3–44

52. Nowak MA, May R (2001) Virus dynamics: mathematical principles of immunology and virology, 1st edn. Oxford University Press, Oxford/New York

53. Smith H, De Leenheer P (2003) Virus dynamics: a global analysis. SIAM J Appl Math 63(4):1313–1327

54. Muldowney JS (1990) Compound matrices and ordinary differential equations. Rocky Mt J Math 20(4):857–872

55. Li M, Muldowney J (1996) A geometric approach to global-stability problems. SIAM J Math Anal 27(4):1070–1083

56. Wang L, Li MY (2006) Mathematical analysis of the global dynamics of a model for HIV infection of CD4+ T cells. Math Biosci 200(1):44–57

57. Ellermeyer S, Wang L (2006) HIV infection and CD4+ T cell dynamics. Discrete Contin Dyn Syst - Ser B 6(6):1417–1430

58. Smith HL (2008) Monotone dynamical systems: an introduction to the theory of competitive and cooperative systems. American Mathematical Society, Providence

59. van den Driessche P, Watmough J (2002) Reproduction numbers and sub-threshold endemic equilibria for

compartmental models of disease transmission. Math Biosci 180:29–48

60. Hutten S, Wälde S, Spillner C, Hauber J, Kehlenbach RH (2009) The nuclear pore component Nup358 promotes transportin-dependent nuclear import. J Cell Sci 122(Pt 8):1100–1110

61. Hutten S, Kehlenbach RH (2006) Nup214 is required for CRM1-dependent nuclear protein export in vivo. Mol Cell Biol 26(18):6772–6785

62. Voit EO (2000) Computational analysis of biochemical systems: a practical guide for biochemists and molecular biologists, 1st edn. Cambridge University Press, New York

63. Carlotti F, Dower SK, Qwarnstrom EE (2000) Dynamic shuttling of nuclear factor kappa B between the nucleus and cytoplasm as a consequence of inhibitor dissociation. J Biol Chem 275(52):41028–41034

64. Lipniacki T, Paszek P, Brasier ARAR, Luxon B, Kimmel M (2004) Mathematical model of NF-kappaB regulatory module. J Theor Biol 228(2):195–215

65. Slice LW, Codner E, Antelman D, Holly M, Wegrzynski B, Wang J, Toome V, Hsu MC, Nalin CM (1992) Characterization of recombinant HIV-1 tat and its interaction with TAR RNA. Biochemistry (Mosc) 31(48):12062–12068

66. Singh J, Padgett RA (2009) Rates of in situ transcription and splicing in large human genes. Nat Struct Mol Biol 16(11):1128–1133

67. Audibert A, Weil D, Dautry F (2002) In vivo kinetics of mRNA splicing and transport in mammalian cells. Mol Cell Biol 22(19):6706–6718

68. Kessler O, Jiang Y, Chasin LA (1993) Order of intron removal during splicing of endogenous adenine phosphoribosyltransferase and dihydrofolate reductase pre-mRNA. Mol Cell Biol 13(10):6211–6222

69. Robert-Guroff M, Popovic M, Gartner S, Markham P, Gallo RC, Reitz MS (1990) Structure and expression of tat-, rev-, and nef-specific transcripts of human immunodeficiency virus type 1 in infected lymphocytes and macrophages. J Virol 64(7):3391–3398

70. Efthymiadis A, Briggs LJ, Jans DA (1998) The HIV-1 tat nuclear localization sequence confers novel nuclear import properties. J Biol Chem 273(3):1623–1628

71. Malim MH, Cullen BR (1991) HIV-1 structural gene expression requires the binding of multiple rev monomers to the viral RRE: implications for HIV-1 latency. Cell 65(2):241–248

72. Daugherty MD, Booth DS, Jayaraman B, Cheng Y, Frankel AD (2010) HIV Rev response element (RRE) directs assembly of the Rev homooligomer into discrete asymmetric complexes. Proc Natl Acad Sci U S A 107(28):12481–12486

73. Mann DA, Mikaélian I, Zemmel RW, Green SM, Lowe AD, Kimura T, Singh M, Butler PJ, Gait MJ, Karn J (1994) A molecular rheostat. Co-operative rev binding to stem I of the rev-response element modulates human immunodeficiency virus type-1 late gene expression. J Mol Biol 241(2):193–207

74. Felber BK, Hadzopoulou-Cladaras M, Cladaras C, Copeland T, Pavlakis GN (1989) Rev protein of human immunodeficiency virus type 1 affects the stability and transport of the viral mRNA. Proc Natl Acad Sci U S A 86(5):1495–1499

75. Kubota S, Duan L, Furuta RA, Hatanaka M, Pomerantz RJ (1996) Nuclear preservation and cytoplasmic degradation of human immunodeficiency virus type 1 rev protein. J Virol 70(2):1282–1287

76. Veloso A, Kirkconnell KS, Magnuson B, Biewen B, Paulsen MT, Wilson TE, Ljungman M (2014) Rate of elongation by RNA polymerase II is associated with specific gene features and epigenetic modifications. Genome Res 24(6):896–905

77. Arava Y, Wang Y, Storey JD, Liu CL, Brown PO, Herschlag D (2003) Genome-wide analysis of mRNA translation profiles in Saccharomyces cerevisiae. Proc Natl Acad Sci U S A 100(7):3889–3894

78. Wada Y, Ohta Y, Xu M, Tsutsumi S, Minami T, Inoue K, Komura D, ‘ichi Kitakami J, Oshida N, Papantonis A, Izumi A, Kobayashi M, Meguro H, Kanki Y, Mimura I, Yamamoto K, Mataki C, Hamakubo T, Shirahige K, Aburatani H, Kimura H, Kodama T, Cook PR, Ihara S (2009) A wave of nascent transcription on activated human genes. Proc Natl Acad Sci U S A 106(43):18357–18361

79. Boireau S, Maiuri P, Basyuk E, de la Mata M, Knezevich A, Pradet-Balade B, Bäcker V, Kornblihtt A, Marcello A, Bertrand E (2007) The transcriptional cycle of HIV-1 in real-time and live cells. J Cell Biol 179(2):291–304

80. Maiuri P, Knezevich A, Bertrand E, Marcello A (2011) Real-time imaging of the HIV-1 transcription cycle in single living cells. Methods San Diego Calif 53(1):62–67

81. Richter S, Cao H, Rana TM (2002) Specific HIV-1 TAR RNA loop sequence and functional groups are required for human cyclin T1-tat-TAR ternary complex formation. Biochemistry (Mosc) 41(20):6391–6397

82. Allen TD, Cronshaw JM, Bagley S, Kiseleva E, Goldberg MW (2000) The nuclear pore complex: mediator of translocation between nucleus and cytoplasm. J Cell Sci 113(Pt 10):1651–1659

83. Grünwald D, Singer RH (2010) In vivo imaging of labelled endogenous β-actin mRNA during nucleocytoplasmic transport. Nature 467(7315):604–607

84. MacKay VL, Li X, Flory MR, Turcott E, Law GL, Serikawa KA, Xu XL, Lee H, Goodlett DR, Aebersold R, Zhao LP, Morris DR (2004) Gene expression analyzed by high-resolution state array analysis and quantitative proteomics: response of yeast to mating pheromone. Mol Cell Proteomics MCP 3(5):478–489

85. Malim MH, Cullen BR (1993) Rev and the fate of pre-mRNA in the nucleus: implications for the regulation of RNA processing in eukaryotes. Mol Cell Biol 13(10):6180–6189

86. Dowling D, Nasr-Esfahani S, Tan CH, O’Brien K, Howard JL, Jans DA, j Purcell DF, Stoltzfus CM, Sonza S (2008) HIV-1 infection induces changes in expression of cellular splicing factors that regulate alternative viral splicing and virus production in macrophages. Retrovirology 5:18

87. Gear CW (1971) The automatic integration of ordinary differential equations. Commun ACM 14(3):176–179

88. Klatt NR, Chomont N, Douek DC, Deeks SG (2013) Immune activation and HIV persistence: implications for curative approaches to HIV infection. Immunol Rev 254(1):326–342

89. Canini L, Perelson AS (2014) Viral kinetic modeling: state of the art. J Pharmacokinet Pharmacodyn 41(5):431–443

90. Banks HT, Flores KB, Hu S, Rosenberg E, Buzon M, Yu X, Lichterfeld M (2015) Immuno-modulatory

strategies for reduction of HIV reservoir cells. J Theor Biol 372:146–158

91. Kumberger P, Frey F, Schwarz US, Graw F (2016) Multiscale modeling of pathogen replication and spread. FEBS Lett
AQ4

92. Mishchenko EL, Bezmaternykh KD, Likhoshvai VA, Ratushny AV, Khlebodarova TM, Yu Sournina N, Ivanisenko VA, Kolchanov NA (2007) Mathematical model for suppression of subgenomic hepatitis C virus RNA replication in cell culture. J Bioinforma Comput Biol 5:593–609

93. Chatterjee A, Smith PF, Perelson AS (2013) Hepatitis C viral kinetics: the past, present, and future. Clin Liver Dis 17(1):13–26

94. Li MY, Shu H (2012) Global dynamics of a mathematical model for HTLV-I infection of CD4+ T cells with delayed CTL response. Nonlinear Anal Real World Appl 13(3):1080–1092

95. Elemans M, Florins A, Willems L, Asquith B (2014) Rates of CTL killing in persistent viral infection in vivo. PLoS Comput Biol 10(4):e1003534

96. Beauchemin CAA, Handel A (2011) A review of mathematical models of influenza a infections within a host or cell culture: lessons learned and challenges ahead. BMC Public Health 11(Suppl 1):S7

97. Murillo LN, Murillo MS, Perelson AS (2013) Towards multiscale modeling of influenza infection. J Theor Biol 332:267–290

98. Manchanda H, Seidel N, Krumbholz A, Sauerbrei A, Schmidtke M, Guthke R (2014) Within-host influenza dynamics: a small-scale mathematical modeling approach. Biosystems 118:51–59

99. Goyal A, Murray JM (2016) Dynamics of in vivo hepatitis D virus infection. J Theor Biol 398:9–19

100. Schiffer JT, Swan DA, Corey L, Wald A (2013) Rapid viral expansion and short drug half-life explain the incomplete effectiveness of current herpes simplex virus 2-directed antiviral agents. Antimicrob Agents Chemother 57(12):5820–5829

101. Carrillo-Bustamante P, Keşmir C, de Boer RJ (2014) Quantifying the protection of activating and inhibiting NK cell receptors during infection with a CMV-like virus. Front Immunol 5:20

102. Fallahi-Sichani M, El-Kebir M, Marino S, Kirschner DE, Linderman JJ (2011) Multiscale computational modeling reveals a critical role for TNF-α receptor 1 dynamics in tuberculosis granuloma formation. J Immunol Baltim Md 1950 186(6):3472–3483

103. Linderman JJ, Kirschner DE (2015) In silico models of M. Tuberculosis infection provide a route to new therapies. Drug Discov Today Dis Models 15:37–41

104. Antia R, Yates A, de Roode JC (2008) The dynamics of acute malaria infections. I. Effect of the parasite's red blood cell preference. Proc Biol Sci 275(1641):1449–1458

105. Adekunle AI, Pinkevych M, McGready R, Luxemburger C, White LJ, Nosten F, Cromer D, Davenport MP (2015) Modeling the dynamics of plasmodium vivax infection and hypnozoite reactivation in vivo. PLoS Negl Trop Dis 9(3):e0003595

106. Schaefer MR, Wonderlich ER, Roeth JF, Leonard JA, Collins KL (2008) HIV-1 Nef targets MHC-I and

CD4 for degradation via a final common beta-COP-dependent pathway in T cells. PLoS Pathog 4(8):e1000131

107. Schwartz O, Maréchal V, Le Gall S, Lemonnier F, Heard JM (1996) Endocytosis of major histocompatibility complex class I molecules is induced by the HIV-1 Nef protein. Nat Med 2(3):338–342

108. Hosseini I, Mac Gabhann F (2012) Multi-scale modeling of HIV infection in vitro and APOBEC3G-based anti-retroviral therapy. PLoS Comput Biol 8(2):e1002371

109. Holmes M, Zhang F, Bieniasz PD (2015) Single-cell and single-cycle analysis of HIV-1 replication. PLoS Pathog 11(6):e1004961

110. Chen B-C, Legant WR, Wang K, Shao L, Milkie DE, Davidson MW, Janetopoulos C, Wu XS, Hammer JA, Liu Z, English BP, Mimori-Kiyosue Y, Romero DP, Ritter AT, Lippincott-Schwartz J, Fritz-Laylin L, Mullins RD, Mitchell DM, Bembenek JN, Reymann A-C, Böhme R, Grill SW, Wang JT, Seydoux G, Tulu US, Kiehart DP, Betzig E (2014) Lattice light-sheet microscopy: imaging molecules to embryos at high spatiotemporal resolution. Science 346(6208):1257998

111. Li D, Shao L, Chen B-C, Zhang X, Zhang M, Moses B, Milkie DE, Beach JR, Hammer JA, Pasham M, Kirchhausen T, Baird MA, Davidson MW, Xu P, Betzig E (2015) ADVANCED IMAGING. Extended-resolution structured illumination imaging of endocytic and cytoskeletal dynamics. Science 349(6251):aab3500

112. Legant WR, Shao L, Grimm JB, Brown TA, Milkie DE, Avants BB, Lavis LD, Betzig E (2016) High-density three-dimensional localization microscopy across large volumes. Nat Methods 13(4):359–365